INFN - Laboratori Nazionali di Frascati, May 1995
From: **The Second DaΦne Physics Handbook**[1]
Chapter 6: Non-Leptonic Kaon Decays
Eds. L. Maiani, G. Pancheri, N. Paver

CP conserving nonleptonic $K \to 3\pi$ decays

L. Maiani
Dipartimento di Fisica, Università di Roma 'La Sapienza'
INFN-Sezione di Roma, Italy 00185

N. Paver
Dipartimento di Fisica Teorica, Università di Trieste
INFN-Sezione di Trieste, Italy 34100

Abstract

The present status of CP conserving $K \to 3\pi$ decays is reviewed. Particular attention is given to the theoretical determinations of the isospin amplitudes and Dalitz plot distributions in the framework of chiral perturbation theory.

1 Modes, branching ratios and expected fluxes

There are, altogether, five distinct CP conserving $K \to 3\pi$ modes, which are listed in Tab. 1 together with their branching ratios and the corresponding number of 'tagged' events obtainable at DAΦNE, with a luminosity of $5 \times 10^{32} cm^{-2}s^{-1}$ in a detector with 4π angular coverage such as KLOE. If, for some channel, 'tagging' is not needed, the corresponding number of events might be larger. The numbers in Tab. 1 are taken from PDG [1], except that (i) the branching ratio of $K_L \to 3\pi^0$ is the most recent determination with the NA31 detector [2], which is three times more precise than previous experiments, and (ii) for the rare decay $K_S \to \pi^+\pi^-\pi^0$, which has not been directly observed yet, the upper and lower

[1]Supported by the INFN, by the EC under the HCM contract number CHRX-CT920026 and by the authors home institutions

Integrated Luminosity: $5 \times 10^{32} cm^{-2} s^{-1} \times 10^7$s		
channel	Br	1 yr DAΦNE
$K^\pm \to \pi^\pm\pi^\pm\pi^\mp$	$5.59 \pm 0.05\%$	5.0×10^8
$K^\pm \to \pi^\pm\pi^0\pi^0$	$1.73 \pm 0.04\%$	1.5×10^8
$K_L \to \pi^+\pi^-\pi^0$	$12.38 \pm 0.21\%$	1.4×10^8
$K_L \to \pi^0\pi^0\pi^0$	$21.6 \pm 0.08\%$	2.4×10^8
$K_S \to \pi^+\pi^-\pi^0$	$\left(3.9^{+5.4+0.9}_{-1.8-0.7}\right) \times 10^{-7}$ $\left(7.8^{+5.7+7.3}_{-4.1-4.9}\right) \times 10^{-7}$	$(3.4 - 6.8) \times 10^2$

Table 1: Experimental $K \to \pi\pi\pi$ branching ratios.

entries are, respectively, the results obtained by the FNAL E621 [3] and the CPLEAR [4] collaborations, by studying the time-dependence of K_L-K_S interference. The number of $K_S \to \pi^+\pi^-\pi^0$ decays expected at DAΦNE is the one implied by the isospin analysis of $K^\pm \to 3\pi$ and $K_L \to 3\pi$ experimental data (assuming $\Delta I \leq 3/2$), which indicates the branching ratio $(2.4 \pm 0.7) \times 10^{-7}$ for this channel [5].

2 Kinematics and Dalitz plot

For the transition

$$K(p) \to \pi_1(p_1)\pi_2(p_2)\pi_3(p_3), \tag{1}$$

one can define the following kinematical invariants:

$$s_i = (p - p_i)^2 = (m_K - m_\pi)^2 - 2m_K T_i, \qquad (i = 1, 2, 3) \tag{2}$$

where T_i are the pion kinetic energies in the kaon rest frame: $\vec{p}_1 + \vec{p}_2 + \vec{p}_3 = 0$ and $E_1 + E_2 + E_3 = m_K$. Since $s_1 + s_2 + s_3 = 3s_0$ with $s_0 = (m_K^2 + 3m_\pi^2)/3$, there are only two independent kinematical variables, which can be defined as

$$Y = \frac{s_3 - s_0}{m_\pi^2}; \qquad X = \frac{s_2 - s_1}{m_\pi^2}. \tag{3}$$

Here, '3' indicates, for a given decay channel, the 'odd charge' pion. We are neglecting pion (and kaon) mass differences, except in the Q-values, that significantly depend on them:

$$Q = T_1 + T_2 + T_3 = m_K - \sum_{i=1}^{3} m_i, \tag{4}$$

and, with an obvious notation referring to the charges of final pion states:

$$Q_{\pm\pm\mp} = 74.9\ MeV; \quad Q_{\pm 00} = 84.1\ MeV; \quad Q^{S,L}_{+-0} = 83.6\ MeV; \quad Q^{S,L}_{000} = 92.8\ MeV. \tag{5}$$

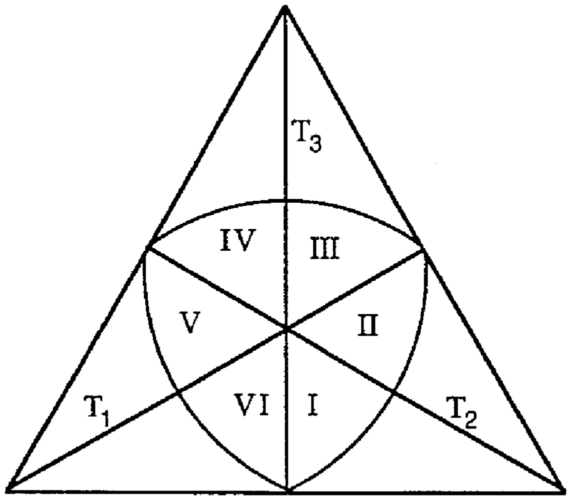

Figure 1: Dalitz plot for $K \to 3\pi$.

In practice, to determine the transition amplitudes from the experimental analysis, in addition to using correct pion and kaon masses, one must account also for isospin breaking and QED corrections.

The Dalitz plot for $K \to 3\pi$ is the equilateral triangle with height Q shown in Fig. 1, where the perpendiculars from internal points (representing the events) to the sides determine the pion kinetic energies, obviously satisfying the energy conservation Eq. (4). Conventionally, the vertical perpendicular refers to the 'odd charge' pion. The centre of the diagram, representing the origin of the three axes at 120° along which one plots T_1, T_2 and T_3, corresponds to the symmetric point $T_1 = T_2 = T_3 = Q/3$. Cartesian coordinates of a point relative to this origin are easily seen to be proportional to the values of Y and of $X/\sqrt{3}$, respectively. All points inside the indicated boundary contour (resulting from three-momentum conservation) are kinematically allowed and represent possible decay events. The diagram is divided into 'sextants', labeled from I to VI, which under permutations of indistinguishable pions are permuted into each other by reflections in the corresponding triangle median.

To evaluate phase space integrals, it is often useful to define Dalitz variables by expressing kinetic energies in terms of polar coordinates r and ϕ, with the origin at the symmetric point [6]:

$$\begin{aligned} T_{1,2} &= \frac{Q}{3}\left(1 + r\cos\left(\frac{2}{3}\pi \mp \phi\right)\right) \\ T_3 &= \frac{Q}{3}\left(1 + r\cos\phi\right). \end{aligned} \tag{6}$$

In Eq. (6): $-\pi < \phi \leq \pi$ and $0 \leq r \leq r(\phi)$, with $r(\phi)$ the boundary curve in the Dalitz

channel	$K^+ \to \pi^+\pi^+\pi^0$	$K^+ \to \pi^+\pi^0\pi^0$	$K_L \to \pi^+\pi^-\pi^0$	$K_L \to \pi^0\pi^0\pi^0$
$\Gamma\,(10^6 s^{-1})$	4.52 ± 0.04	1.40 ± 0.032	2.39 ± 0.04	4.19 ± 0.16
$g\,(10^{-1})$	-2.154 ± 0.035	5.94 ± 0.19	6.70 ± 0.14	–
$h\,(10^{-2})$	1.2 ± 0.8	3.5 ± 1.5	7.9 ± 0.7	$-0.33 \pm 0.11 \pm 0.07$
$k\,(10^{-2})$	-1.01 ± 0.34	–	0.98 ± 0.18	–

Table 2: Experimental values of widths and Dalitz plot slopes for $K \to 3\pi$ [1].

plot, implicitly defined, for equal pion masses, by the equation

$$1 - (1+\alpha)r^2 - \alpha r^3 \cos 3\phi = 0, \tag{7}$$

with $\alpha = (2Q/m_K)\,(2-(Q/m_K))^{-2}$. In the approximation of neglecting α, which actually is of the order of 0.1, the limiting curve in the plot would become a circle. Moreover, the variables X and Y defined in (3) are expressed in terms of polar coordinates as

$$Y = -\frac{2}{3}\frac{m_K}{m_\pi^2}Q\,r\cos\phi, \qquad X = \frac{2}{\sqrt{3}}\frac{m_K}{m_\pi^2}Q\,r\sin\phi, \tag{8}$$

so that the plot in terms of Y and $X/\sqrt{3}$ is quite similar to Fig. 1 (except from the maximum radius of the contour of the allowed region, which in this case is obviously different).

The decay rates are expressed in terms of polar variables as

$$\Gamma(K \to 3\pi) \equiv \frac{1}{(4\pi)^3 m_K}\frac{\sqrt{3}}{18}Q^2 \int\int r\,dr\,d\phi |A(r,\phi)|^2, \tag{9}$$

where the integration is over the full Dalitz plot. Such integration, as well as integrations over the Dalitz plot with cuts, becomes particularly simple in the limit $\alpha = 0$ in (7), which in many cases represents a good approximation. Explicit calculations of a set of relevant Dalitz plot integrals, also with cuts, can be found in the Appendix of Ref. [7].

Since the maximum allowed pion kinetic energies are rather small ($T_{i,max} \simeq 50\ MeV$), it is natural to expand Dalitz plot distributions in powers of Y and X:

$$|A(K \to 3\pi)|^2 \propto 1 + gY + jX + hY^2 + kX^2, \tag{10}$$

where, actually, CP conservation implies $j = 0$. The experimental data do not require higher powers than included in (10), and the determinations of Γ, g, h and k for the different $K \to 3\pi$ modes are listed in Tab. 2. As one can see, present accuracies are at % level or better (depending on the different decay channels) for the widths Γ and the linear slopes g, but are somewhat worse (in general much larger than 10%) for the quadratic slopes h and k.

3 $K \to 3\pi$ isospin amplitudes

Consistent with Eq. (10), also the $K \to 3\pi$ transition amplitudes are expanded in power series of the variables X and Y around the centre of the Dalitz plot $X = Y = 0$, assuming the absence of nearby poles, up to quadratic terms. Limiting to $\Delta I = 1/2$ and $\Delta I = 3/2$ transitions, as also consistent with experimental data, there are three possible three-pion final states with definite isospin: $|(3\pi)_{I=1}, symm.>$; $|(3\pi)_{I=1}, mixed\ symm.>$; and $|(3\pi)_{I=2}>$. Due to the Bose symmetry of the three-pion final state, the transition (of the K_S) to the $I = 0$ state, although possible in principle, is strongly suppressed by a high angular momentum centrifugal barrier, and we ignore it. Neglecting isospin breaking effects, the general Bose-symmetric and CP conserving expansion can be written in terms of five independent weak amplitudes as [8, 9]:

$$
\begin{aligned}
A_{++-} &\equiv A(K^+ \to \pi^+\pi^+\pi^-) = 2A_c(s_1, s_2, s_3) + B_c(s_1, s_2, s_3) + B_2(s_1, s_2, s_3) \\
A_{00+} &\equiv A(K^+ \to \pi^0\pi^0\pi^+) = A_c(s_1, s_2, s_3) - B_c(s_1, s_2, s_3) + B_2(s_1, s_2, s_3) \\
A^L_{+-0} &\equiv A(K_L \to \pi^+\pi^-\pi^0) = A_n(s_1, s_2, s_3) - B_n(s_1, s_2, s_3) \\
A^L_{000} &\equiv A(K_L \to \pi^0\pi^0\pi^0) = 3A_n(s_1, s_2, s_3) \\
A^S_{+-0} &\equiv A(K_S \to \pi^+\pi^-\pi^0) = \frac{2}{3}\left[B_2(s_3, s_2, s_1) - B_2(s_1, s_3, s_2)\right].
\end{aligned} \tag{11}
$$

In Eq. (11), $A_{c,n}$ are completely symmetric under permutations of the indices 1, 2 and 3. Conversely, $B_{c,n,2}$ are symmetric only under the exchange $1 \leftrightarrow 2$, and under permutations of indices obey the relation

$$
B_j(s_1, s_2, s_3) + B_j(s_3, s_2, s_1) + B_j(s_1, s_3, s_2) = 0. \tag{12}
$$

Finally, the amplitude for $K_S \to \pi^+\pi^-\pi^0$ is antisymmetric under the exchange $1 \leftrightarrow 2$. From the isospin point of view, the amplitudes $A_{c,n}$ and $B_{c,n}$ contribute to $\Delta I = 1/2$ and $\Delta I = 3/2$ transitions to the $I = 1$ final state, while B_2 is the pure $\Delta I = 3/2$ transition to $I = 2$. Also, one should notice that there are two kinds of amplitudes to final $I = 1$, which reflect the different pion exchange symmetry properties of the corresponding three-pion states, i.e., the fully symmetric A's and the B's with mixed symmetry.

Taking the symmetry properties into account, A's and B's can be expanded up to quadratic terms in X and Y as follows:

$$
\begin{aligned}
A_j &= a_j + c_j\left(Y^2 + X^2/3\right) \\
B_j &= b_j Y + d_j\left(Y^2 - X^2/3\right).
\end{aligned} \tag{13}
$$

In the absence of final state strong interactions, the CP conserving amplitudes in (11) and (13) could be taken as real. As required by unitarity, strong interaction rescattering of final state pions produce imaginary parts, which can be taken into account by introducing more phenomenological parameters (in addition to a_j, b_j, c_j and d_j) in Eq. (13). Due to the smallness of the available $K \to 3\pi$ phase space, these effects are expected to be small and, to avoid too many free parameters, in current fits to the data such strong phases have been assumed to be negligible (within an uncertainty of 15°). This assumption is consistent with the available experimental information, and also with theoretical expectations [5, 10].

Nevertheless, as being sensitive to the properties of low-energy meson dynamics, rescattering effects are theoretically quite interesting and could eventually be in the reach of next-generation, high precision experiments on $K \to 3\pi$. Consequently, their measurement would provide alternative, and stringent, tests of the relevant theoretical description. Specifically, of the pion-pion interaction if one neglects irreducible 3π rescattering diagrams that should be phase space-suppressed (barring anomalously large 3π vertices). Such tests would involve the really low-energy range, where the framework of chiral perturbation theory (χPT) can be most reliably applied. Another, and very important, point of interest is the fact that these imaginary parts crucially enter the determination of direct CP-violating asymmetries in $K \to 3\pi$ decays, and consequently are relevant to searches for this, still unclear, phenomenon in a channel alternative to $K \to 2\pi$ [11].

Phenomenologically, momentum dependence of rescattering should be taken into account for a consistent low-energy expansion of the amplitudes. This is desirable also in view of the momentum expansions predicted by chiral perturbation theory, which will be described in the sequel. For the parametrization of such effects, there is the complication that the two final $I = 1$ three-pion states are coupled by (isospin conserving) strong interactions, so that they can mix. This situation can be dealt with, rather generally, by a coupled-channel formalism that introduces, in the $I = 1$ sector, a two-dimensional, momentum-dependent rescattering matrix R common to both charged and neutral kaon decays, connecting symmetric and nonsymmetric amplitudes [12]. Since $R = I$ corresponds to the limiting case of no final state interaction, R can be expanded as $R = I + i\mathcal{R}$, where the elements of the (real) matrix $\mathcal{R}$ are functions of X and Y. Such functions can be expanded around the centre of the Dalitz plot, similar to Eq. (13), and are expected to be small over the whole allowed kinematical region. Moreover, in general the R-matrix elements are not all independent, but are related by unitarity constraints following from probability conservation.

Contrary to the $I = 1$ case, for the decays to the $I = 2$ three-pion state, which is unique and cannot mix with the others *via* strong interactions, there is just one amplitude with definite symmetry properties, and final state interactions are simply taken into account by a phase function that is unique for all decay modes, similar to the case of $K \to 2\pi$ where $I = 0$ and $I = 2$ final states do not mix.

For simplicity, one can limit to include rescattering effects only in the constant and linear slopes in Eq. (13), as it seems justified by the smallness of experimental quadratic slopes. In that case, using Eq. (13), the expansion of Eq. (11) around $X = Y = 0$ takes on the form:[2]

$$
\begin{aligned}
A_{++-} &= 2a_c\left(1 + i\alpha_0 + i\alpha_0' Y/2\right) + \left[b_c\left(1 + i\beta_0\right) + b_2\left(1 + i\delta_0\right)\right] Y \\
&+ 2c_c\left(Y^2 + X^2/3\right) + \left(d_c + d_2\right)\left(Y^2 - X^2/3\right) \\
A_{00+} &= a_c\left(1 + i\alpha_0 - i\alpha_0' Y\right) - \left[b_c\left(1 + i\beta_0\right) - b_2\left(1 + i\delta_0\right)\right] Y
\end{aligned}
$$

[2] A general presentation, and a discussion in the framework of χPT, can be found in Ref. [12].

$$
\begin{aligned}
& + \quad c_c \left(Y^2 + X^2/3\right) - (d_c - d_2) \left(Y^2 - X^2/3\right) \\
A^L_{+-0} &= a_n \left(1 + i\alpha_0 - i\alpha_0' Y\right) - b_n \left(1 + i\beta_0\right) Y \\
& + \quad c_n \left(Y^2 + X^2/3\right) - d_n \left(Y^2 - X^2/3\right) \\
A^L_{000} &= 3a_n \left(1 + i\alpha_0\right) + 3c_n \left(Y^2 + X^2/3\right) \\
A^S_{+-0} &= -(2/3) b_2 \left(1 + i\delta_0\right) X + (4/3) d_2 XY. \qquad (14)
\end{aligned}
$$

The amplitudes for the decays of the K^- are determined by taking complex-conjugates of the coefficients $a, \ldots, d$ with unchanged strong interaction imaginary parts. CP conservation implies that these coefficients should be real and consequently, in this case, the amplitudes for K^+ and K^- decays must be the same. In the presence of CP violation, the coefficients $a, \ldots, d$ are in general complex, so that amplitudes for charge-conjugate processes can be different. Furthermore, in this situation the $K_S \to \pi^+\pi^-\pi^0$ amplitude could get additional, imaginary constant and linear (in Y) terms, while an imaginary amplitude linear in X could appear in $K_L \to \pi^+\pi^-\pi^0$ [13].

A representation alternative to (14), which has been adopted in fits to experimental data [5, 10], is the expansion in terms of amplitudes with definite isospin selection rules. With $\Delta I \le 3/2$, neglecting strong interaction imaginary parts, such an expansion can be written as

$$
\begin{aligned}
A_{++-} &= (2\alpha_1 - \alpha_3) + \left[(\beta_1 - \beta_3/2) + \sqrt{3}\gamma_3\right] Y \\
& + \quad 2(\zeta_1 + \zeta_3) \left(Y^2 + X^2/3\right) - (\xi_1 + \xi_3 - \xi_3') \left(Y^2 - X^2/3\right) \\
A_{00+} &= -(\alpha_1 - \alpha_3/2) + \left[(\beta_1 - \beta_3/2) - \sqrt{3}\gamma_3\right] Y \\
& - \quad (\zeta_1 + \zeta_3) \left(Y^2 + X^2/3\right) - (\xi_1 + \xi_3 + \xi_3') \left(Y^2 - X^2/3\right) \\
A^L_{+-0} &= (\alpha_1 + \alpha_3) - (\beta_1 + \beta_3) Y \\
& + \quad (\zeta_1 - 2\zeta_3) \left(Y^2 + X^2/3\right) + (\xi_1 - 2\xi_3) \left(Y^2 - X^2/3\right) \\
A^L_{000} &= -3(\alpha_1 + \alpha_3) - 3(\zeta_1 - 2\zeta_3) \left(Y^2 + X^2/3\right) \\
A^S_{+-0} &= (2/\sqrt{3})\gamma_3 X - (4/3)\xi_3' XY. \qquad (15)
\end{aligned}
$$

In Eq. (15), the subscripts 1 and 3 refer to $\Delta I = 1/2$ and $\Delta I = 3/2$, respectively. The relation between the amplitudes in Eq. (14) and those in Eq. (15) is easily found to be:[3]

$$
\begin{array}{ll}
a_c = -\alpha_1 + \alpha_3/2 & a_n = \alpha_1 + \alpha_3 \\
b_c = -\beta_1 + \beta_3/2 & b_n = \beta_1 + \beta_3 \\
c_c = -\zeta_1 - \zeta_3 & c_n = \zeta_1 - 2\zeta_3 \\
d_c = \xi_1 + \xi_3 & d_n = -\xi_1 + 2\xi_3 \\
b_2 = -\sqrt{3}\gamma_3 & d_2 = -\xi_3'.
\end{array} \qquad (16)
$$

In conclusion, the complex of $K \to 3\pi$ modes is described by the set of ten independent (real) isospin amplitudes in Eq. (15), which are collected in Tab. 3 for convenience, or

[3] Notice that different isospin phase conventions are adopted in Refs. [5] and [12].

alternatively by the ten amplitudes in Eq. (14). There are, in addition, the imaginary parts from final state strong interactions, parametrized in leading order by four real constants, as in Eq. (14).

	constant	linear	quadratic
$\Delta I = 1/2$	α_1	β_1	ξ_1, ζ_1
$\Delta I = 3/2$	α_3	β_3, γ_3	ξ_3, ξ_3', ζ_3

Table 3: Independent isospin amplitudes for $K \to \pi\pi\pi$

4 Experimental determinations

Since both kaons and pions are spinless, all observables (and therefore the information on the decay dynamics) are embodied in the Dalitz plot distributions (10), i.e., in the decay rates and in the linear and quadratic slopes for the different channels. From these, one has to separately determine the coefficients of the amplitude expansions in Eq. (15), in order to compare them with theoretical predictions. In principle, in the CP conserving case, there are fifteen experimentally measurable numbers from Dalitz plots (four for each of the modes $K^+ \to \pi^+\pi^+\pi^-$, $K^+ \to \pi^+\pi^0\pi^0$ and $K_L \to \pi^+\pi^-\pi^0$, two for the mode $K_L \to 3\pi^0$ and one for $K_S \to \pi^+\pi^-\pi^0$), from which to determine the isospin amplitudes. In particular, once measured, the branching ratio $Br(K_S \to \pi^+\pi^-\pi^0)$ directly determines the absolute value of the $\Delta I = 3/2$ amplitude γ_3 (up to ξ_3').

In Tabs. 4 and 5 (located for convenience in Sec. 5.1) we report the results of the joint fit of $K \to 2\pi$ and $K \to 3\pi$ isospin amplitudes to the available experimental data, performed in Ref. [5],[4] updating the analysis of Ref. [10].

Tab. 4 indicates the present level of accuracy on the amplitudes in Eq. (15): in general, $\Delta I = 3/2$ amplitudes are not so well-determined, compared to the dominant $\Delta I = 1/2$ ones. Specifically, for stringent tests of the chiral Lagrangian description of $K \to 3\pi$, the linear coefficient β_3 is not determined as accurately as one would wish, and the knowledge of quadratic coefficients, representing genuine predictions from the next-to-leading order in the chiral expansion, is generally poor.

5 Theoretical predictions

Due to the low kinetic energy available to final state pions, $K \to 3\pi$ seems the ideal process where to apply the notion of the Goldstone-boson nature of pseudoscalar mesons, and the related low-energy expansions of transition amplitudes, that are obtained from the chiral Lagrangian realization of the nonleptonic $\Delta S = 1$ weak interaction. Such a Lagrangian,

[4]Actually, the fit of [5] is prior to the recent determinations of the quadratic slope h for $K_L \to 3\pi^0$ [14], which is uncorrelated from constant and linear slopes, and of $\Gamma(K_L \to 3\pi^0)$ [2]. These experimental results could significantly improve the fit.

$\Delta I = 1/2$			
α_1	β_1	ζ_1	ξ_1
91.71 ± 0.32	-25.68 ± 0.27	-0.47 ± 0.15	-1.51 ± 0.30

$\Delta I = 3/2$					
α_3	β_3	γ_3	ζ_3	ξ_3	ξ_3'
-7.36 ± 0.47	-2.43 ± 0.41	2.26 ± 0.23	-0.21 ± 0.08	-0.12 ± 0.17	-0.21 ± 0.51

Table 4: Determinations of $K \to 3\pi$ isospin amplitudes, in units 10^{-8}.

written in terms of Goldstone boson-pseudoscalar meson fields π, K and η, has the same transformation properties under unitary symmetry as the four-quark Lagrangian originally derived in the framework of the short distance operator product expansion, and automatically accounts for general properties of non-perturbative strong interactions governed by long-distance QCD. By the feature of the Goldstone boson interaction, of vanishing in the zero four-momentum limit, this formalism leads to amplitudes expansions in powers of pseudoscalar meson masses and energies which, in particular, naturally incorporate the current algebra soft-pion theorems. These theorems are rigorously valid in the chiral symmetry limit and, in the specific case of kaon nonleptonic decays, relate $K \to 3\pi$ to $K \to 2\pi$ amplitudes making use solely of the chiral $SU(3)_L \times SU(3)_R$ transformation properties (as a right-handed singlet) of the nonleptonic weak hamiltonian [15]. They can be written symbolically, with $F_\pi = 93.3\,MeV$ the pion decay constant, as:

$$\lim_{p_3 \to 0} \langle \pi(p_1)\pi(p_2)\pi(p_3)|\mathcal{L}_W^{p.c.}|K\rangle = \frac{-i}{F_\pi}\langle \pi(p_1)\pi(p_2)|\mathcal{L}_W^{p.v.}|K\rangle, \tag{17}$$

where $p.c.$ and $p.v.$ mean parity-conserving and parity-violating components, and similar relations hold for the other pions becoming soft and for the different decay channels. Actually, soft-pion points are somewhat far from the kinematically allowed region of the Dalitz plot, where mesons have small, but finite, four-momenta. Thus, in addition to providing a general, and convenient, computational tool to evaluate the relevant hadronic matrix elements of $\mathcal{L}_W$ directly in terms of Feynman diagrams with pion, kaon and eta fields, one advantage of the effective chiral Lagrangian approach is that it gives a consistent, unambiguous prescription to extrapolate soft-pion theorem predictions into the physical region.

Actually, such a Lagrangian depends on a number of phenomenological coupling constants (increasing with the desired order in the momentum expansion), whose values cannot be predicted theoretically from the symmetry but, instead, must be inferred from experiment. To account for both the leading $O(p^2)$ and the next-to-leading $O(p^4)$ corrections in the χPT expansion, a considerable number of such constants are needed. Fortunately, this number is limited enough for the scheme to remain predictive, and to be severely tested by accurate experimental data on $K \to 2\pi$ and $K \to 3\pi$. In the next section, we briefly review the application of χPT to $K \to 3\pi$.

5.1 Chiral perturbation theory

For convenience, we recall the Standard Model non-leptonic weak effective Lagrangian in terms of quark fields [16]:

$$\mathcal{L}_W(\Delta S = 1) = \frac{G_F}{\sqrt{2}} V_{ud} V_{us}^* \sum_i C_i(\mu) Q_i(\mu) + h.c., \tag{18}$$

where $C_i(\mu)$ are numerical coefficients depending on heavy masses and calculable in perturbative QCD, and $Q_i(\mu)$ are local four-quark operators with $\Delta S = 1$ and $\Delta I = 1/2,\ 3/2$ [17]. Both C_i and Q_i depend on a renormalization scale μ, but their product must be μ-independent to ensure independence of physical amplitudes from this scale.

To make theoretical predictions, and thus compare the quark-level transition Lagrangian (18) with experimental data, one must estimate matrix elements of the four-quark operators between initial $|K\rangle$ and final $\langle 2\pi|$ and $\langle 3\pi|$ hadronic states. These matrix elements crucially depend on the nonperturbative structure of low-energy QCD, so that calculations relying on different hadronization schemes should be model dependent. The chiral Lagrangian technique provides a general framework for such matrix elements, and is essentially based on the transformation properties of the operators in Eq. (18) under separate $SU(3)$ rotations of left-handed and of right-handed fields, i.e. the chiral $SU(3)_L \times SU(3)_R$ symmetry transformations (g_L, g_R).

At the scale $\mu < m_c$, the basis of operators can be chosen as $(q_{L,R} = \frac{1}{2}(1 - \gamma_5) q)$:

$$\begin{aligned}
Q_1 &= 4\bar{s}_L\gamma_\mu d_L \bar{u}_L\gamma^\mu u_L, \quad Q_2 = 4\bar{s}_L\gamma_\mu u_L \bar{u}_L\gamma^\mu d_L, \quad Q_3 = 4\bar{s}_L\gamma_\mu d_L \sum_{q=u,d,s} \bar{q}_L\gamma^\mu q_L, \\
Q_5 &= 4\bar{s}_L\gamma_\mu d_L \sum_{q=u,d,s} \bar{q}_R\gamma^\mu q_R, \qquad Q_6 = -8 \sum_{q=u,d,s} \bar{s}_L q_R \bar{q}_R d_L, \\
Q_7 &= 6\bar{s}_L\gamma_\mu d_L \sum_{q=u,d,s} e_q \bar{q}_R\gamma^\mu q_R, \qquad Q_8 = -12 \sum_{q=u,d,s} e_q \bar{s}_L q_R \bar{q} d_L,
\end{aligned} \tag{19}$$

where color indices are implicitly contracted within each quark-bilinear factor. The '$V - A$' operators Q_1 and Q_2 have selection rule $\Delta I = 1/2,\ 3/2$ and behave as $(8_L, 1_R) + (27_L, 1_R)$; the penguin operators Q_3, Q_5 and Q_6 are purely $\Delta I = 1/2$, and transform as $(8_L, 1_R)$; the electroweak penguin operators Q_7 and Q_8 transform as $(8_L, 8_R)$, and have both $\Delta I = 1/2$ and $\Delta I = 3/2$ components. Electropenguin operators are suppressed by a small coefficient of order α_{QED}, so they must be considered only in the CP violating case [11].

Accordingly, limiting to the operators $Q_1, \ldots, Q_6$, the lowest order, $O(p^2)$, weak chiral Lagrangian is the sum of a $(8_L, 1_R)$ operator plus a $(27_L, 1_R)$ one, whose forms are uniquely dictated by chiral symmetry [18]:

$$\mathcal{L}_W^{(2)}|_{(8,1)+(27,1)} = c_2\, Tr\lambda_6 L_\mu L^\mu + c_3\, t^{jl}_{ik} (Tr Q^i_j L_\mu)(Tr Q^k_l L^\mu). \tag{20}$$

Here, $L_\mu = iU^\dagger\partial_\mu U$ with $U = \exp(i\sqrt{2}\Phi/F_\pi)$, and Φ is the pseudoscalar meson $SU(3)$

matrix, so that U transforms under (g_L, g_R) as $U \to g_L U g_R^\dagger$ [19]:

$$\Phi = \frac{1}{\sqrt{2}} \sum_{i=1,\cdots,8} \lambda_i \Pi_i = \begin{pmatrix} \frac{\pi^0}{\sqrt{2}} + \frac{\eta}{\sqrt{6}} & -\pi^+ & -K^+ \\ \pi^- & -\frac{\pi^0}{\sqrt{2}} + \frac{\eta}{\sqrt{6}} & -K^0 \\ K^- & -\bar{K}^0 & -\frac{2}{\sqrt{6}}\eta \end{pmatrix} \tag{21}$$

The matrices Q^i_j and the coefficients t^{jl}_{ik} that appear in (20) can be found, e.g., in [20, 5]. The octet and 27-plet coupling constants c_2 and c_3, the only two parameters needed at order p^2 in χPT, cannot be estimated theoretically, but must be phenomenologically fitted from experimental data.

$K \to 2\pi$ and $K \to 3\pi$ amplitudes at order p^2 are obtained from the 'tree' diagrams in Fig. 2, where the needed weak vertices are obtained by expanding the effective Lagrangian (20) to the right number of pseudoscalar meson fields. As shown in Fig. 2, in the case of $K \to 3\pi$ also 'pole diagrams' appear, which involve the four-meson strong interaction. At the order p^2, this is represented by the chiral Lagrangian [21, 19]

$$\mathcal{L}_S^{(2)} = \frac{F_\pi^2}{4} Tr \left[\partial_\mu U \partial^\mu U^\dagger + 2B\mathcal{M}\left(U^\dagger + U\right)\right], \tag{22}$$

where $\mathcal{M} = \mathrm{diag}(m_u, m_d, m_s)$ is the quark mass matrix, explicitly breaking chiral symmetry, and B is a constant such that, to leading order, $2B\mathcal{M} = \mathrm{diag}(m_\pi^2, m_\pi^2, 2m_K^2 - m_\pi^2)$ in the $SU(2)$ limit.

Defining $K \to 2\pi$ amplitudes as $A_0 = i a_{1/2} \exp(i\delta_0)$ and $A_2 = -i a_{3/2} \exp(i\delta_2)$, with the usual isospin decomposition

$$\begin{aligned} A(K^+ \to \pi^+\pi^0) &= (\sqrt{3}/2) A_2 \\ A(K^0 \to \pi^0\pi^0) &= \sqrt{1/3}A_0 + \sqrt{2/3}A_2 \\ A(K^0 \to \pi^+\pi^-) &= -\sqrt{1/3}A_0 + \sqrt{1/6}A_2, \end{aligned} \tag{23}$$

the diagrams in Fig. 2 directly give for the $\Delta I = 1/2$ amplitudes:

$$\begin{aligned} a_{1/2} &= \frac{1}{F_\pi^2 F_K} \sqrt{6} \left(m_K^2 - m_\pi^2\right) \left(c_2 - \frac{2}{3}c_3\right) \\ \alpha_1 &= \frac{1}{F_\pi^3 F_K} \frac{m_K^2}{3} \left(c_2 - \frac{2}{3}c_3\right) \\ \beta_1 &= \frac{1}{F_\pi^3 F_K} \left(-m_\pi^2\right) \left(c_2 - \frac{2}{3}c_3\right), \end{aligned} \tag{24}$$

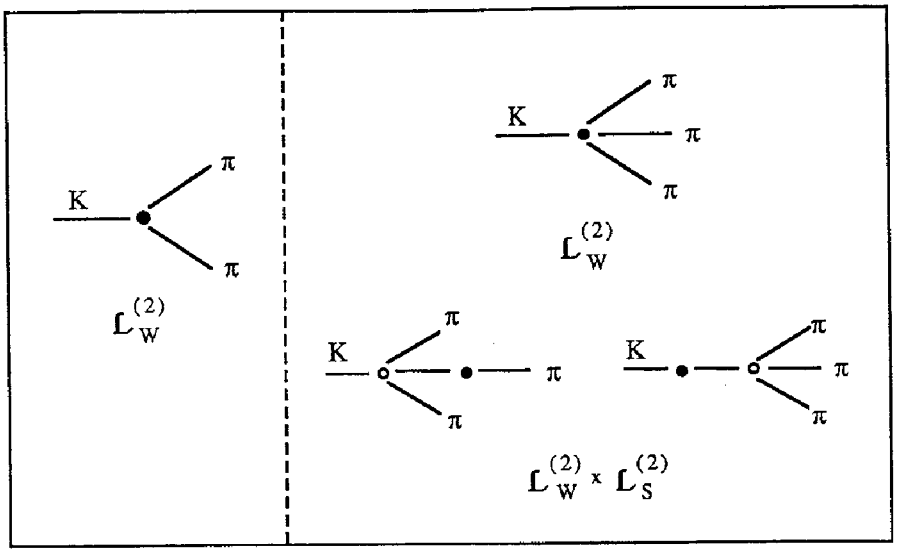

Figure 2: Lowest order diagrams ($O(p^2)$) for $K \to 2\pi$ and $K \to 3\pi$: the weak vertex is represented by •, the strong one by ∘.

and for the $\Delta I = 3/2$ amplitudes:

$$\begin{aligned}
a_{3/2} &= \frac{1}{F_\pi^2 F_K}\left(m_K^2 - m_\pi^2\right)\left(-\frac{20}{\sqrt{3}}c_3\right) \\
\alpha_3 &= \frac{1}{F_\pi^3 F_K} m_K^2 \left(\frac{20}{9}c_3\right) \\
\beta_3 &= \frac{1}{F_\pi^3 F_K}\frac{m_\pi^2}{m_K^2 - m_\pi^2}\left(5m_K^2 - 14m_\pi^2\right)\left(\frac{5}{3}c_3\right) \\
\gamma_3 &= \frac{1}{F_\pi^3 F_K}\frac{m_\pi^2}{m_K^2 - m_\pi^2}\left(3m_K^2 - 2m_\pi^2\right)\left(\frac{-15}{2\sqrt{3}}c_3\right).
\end{aligned} \tag{25}$$

Although, in principle, at this level $F_\pi = F_K = F_0$, $SU(3)$ breaking is phenomenologically included by using $F_K \cong 1.22\ F_\pi$.

As anticipated, Eqs. (24) and (25) manifestly express the current algebra soft-pion theorems relating $K \to 3\pi$ amplitudes with vanishing pion four-momentum to $K \to 2\pi$ ones, and also include finite pion mass corrections extrapolating those relations back into the physical region.

Indeed, the values of the coupling constants c_2 and c_3 can be obtained by fitting (24) and (25) to the experimental $K \to 2\pi$ amplitudes. The results, displaying the $\Delta I = 1/2$ enhancement in $K \to 2\pi$, are shown in the third column of Tab. 5.

The so determined constants c_2 and c_3 can be used in Eqs. (24) and (25) to predict

	exp. fit	χPT O(p^2)	χPT O(p^4) [5]	Units
$a_{1/2}$	0.4699 ± 0.0012	0.4698 (input)	0.4698 (input)	KeV
$a_{3/2}$	0.0211 ± 0.0001	0.0211 (input)	0.0211 (input)	KeV
$\delta_2 - \delta_0$	-61.5 ± 4	0	-29	degrees
c_2/F_π^2		0.95	0.662 ± 0.005	10^{-7}
c_3/F_π^2		-0.009	-0.0083 ± 0.0002	10^{-7}

Table 5: Isospin amplitudes and relative phase for $K \to 2\pi$.

Units 10^{-8}					
	$O(p^2)$	$O(p^4)$		$1/N_c$ $O(p^4)$	
	Eqs. (24)-(25)	Ref. [5]	Ref. [25]	Ref. [35]	Ref. [36]
α_1	74.0	91.8	input	88.8	92
β_1	-16.5	-25.6	input	-26.5	-26
ζ_1	–	-0.6	-0.47 ± 0.18	-0.22	-0.2
ξ_1	–	-1.5	-1.58 ± 0.19	-0.88	-0.8
α_3	-4.1	-7.6	input	-5.6	-5.9
β_3	-1.0	-2.5	input	-1.9	-1.4
γ_3	1.8	2.5	input	2.5	2.4
ζ_3	–	-0.02	$-0.011 \pm .006$	-0.007	-0.01
ξ_3	–	-0.05	0.092 ± 0.030	0.018	0.0
ξ_3'	–	-0.08	-0.033 ± 0.077	-0.081	–

Table 6: Theoretical predictions for $K \to 3\pi$ isospin amplitudes.

the $K \to 3\pi$ isospin amplitudes at $O(p^2)$.[5] These predictions are reported in the second column of Tab. 6. Comparing with the numbers in Tab. 4, one can see that the order p^2 is in reasonable agreement with the data, as it underestimates the experimental amplitudes, on the average, by about 20-35%. This is not surprising, as the expected size of next-to-leading corrections, of order p^4, is $m_K^2/(4\pi F_\pi)^2 \sim 0.2$, where $4\pi F_\pi \simeq 1\,GeV$ is the scale of chiral symmetry breaking. We should also remark, from Tab. 4, that the amplitude α_1 is so well measured that it really represents a challenge to the theory. On the other hand, the discrepancy of the theoretical prediction with the central value of the $\Delta I = 3/2$ slope β_3 seems rather sizable. Consequently, it would be desirable to significantly improve the experimental accuracy on this parameter. We remark, also, that both the final state strong interaction phases and the quadratic slopes vanish at this order in χPT, reflecting, respectively, the 'tree' diagram approximation of Fig. 2 where there are no absorptive parts, and the use of the two-derivative Lagrangian (20) which cannot provide enough powers in momenta.

The deviations of the $O(p^2)$ predictions from the experimental values of constant and

[5]If, conversely, one attempted to infer c_2 and c_3 from $K \to 3\pi$ data, the determination of c_2 would remain consistent with that in Tab. 5, whereas that of c_3 would change considerably [22].

linear amplitudes, and the evidence for non-vanishing quadratic slopes, call for the introduction of the next-to-leading chiral corrections. The general form of the $\Delta S = 1$ non-leptonic Lagrangian at order p^4, $\mathcal{L}_W^{(4)}$, was worked out in Ref. [20]. The number of new independent local operators, allowed by the symmetry to contribute to $\mathcal{L}_W^{(4)}$, whose coupling constants are not determined theoretically, is in general unmanageably large. In this set, there are four-derivative operators, which contribute X^2 and Y^2 terms to $K \to 3\pi$ matrix elements and thus determine the quadratic slopes in Eqs. (14) or (15), such as the $\Delta I = 1/2$ operators of the form [23]:

$$O_1^{(4)} = \langle \lambda_6 L_\mu L^\mu L_\nu L^\nu \rangle, \qquad O_2^{(4)} = \langle \lambda_6 L_\mu L_\nu L^\mu L^\nu \rangle, \tag{26}$$

and others. There are, also, a multitude of operators with higher derivatives of meson fields, *etc.*.

Four-derivative operators obviously vanish at soft-pion points and thus cannot contribute to $K \to 2\pi$, so that no information on them can be derived from the $K \to 2\pi$ sector, as it is the case of c_2 and c_3 at the leading order p^2. On the other hand, apart from (small) corrections of order m_π^2/m_K^2, higher order operators contributing to both $K \to 3\pi$ and $K \to 2\pi$, but not contributing X^2 and Y^2 terms, preserve the leading order relations between $K \to 3\pi$ and $K \to 2\pi$. Consequently, they can be absorbed in the definition of the physical $K \to 2\pi$ amplitudes or, equivalently, in a redefinition of the coupling constants c_2 and c_3.

It turns out that for $K \to 2\pi$ and $K \to 3\pi$ decays the situation considerably simplifies, because only seven linear combinations of the possible $O(p^4)$ local operators in $\mathcal{L}_W^{(4)}$ are found to be active in these processes [5]. The discussion of the analogous, order p^4, weak Lagrangian for non-leptonic radiative kaon decays, and a presentation of the relevant phenomenology, can be found in Ref. [24].

Specifically, denoting by A_i any of the $K \to 2\pi$ and $K \to 3\pi$ amplitudes up to order p^4, we have

$$A_i = A_i^{(2)} + A_i^{(4)}, \tag{27}$$

where $A_i^{(2)}$ is the leading order, and $A_i^{(4)}$ is the next-to-leading correction. As pictorially represented in Fig. 3, the latter can be decomposed as:

$$A_i^{(4)} = A_{i,loop}(\mu) + A_{i,ct}^w(\mu) + A_{i,poles}. \tag{28}$$

In Eq. (28), $A_{i,loop}$ represents the contribution from chiral loop diagrams,[6] and $A_{i,ct}^w$ accounts for the tree diagram $O(p^4)$ weak counterterm contributions in Fig. 3, connected to the above mentioned higher dimension operators determining $\mathcal{L}_W^{(4)}$, with *a priori* unknown low-energy coupling constants to be determined phenomenologically from data on $K \to 2\pi$ and $K \to 3\pi$. In addition, there appear a number of $O(p^4)$ strong interaction counterterms, which determine $\mathcal{L}_S^{(4)}$ needed in the pole diagrams of Fig. 3, but these constants are

[6] 'Tadpole-like' diagrams, with loops correcting the individual $\mathcal{L}_W^{(2)}$ and $\mathcal{L}_S^{(2)}$ vertices of Fig. 2, are not depicted in Fig. 3.

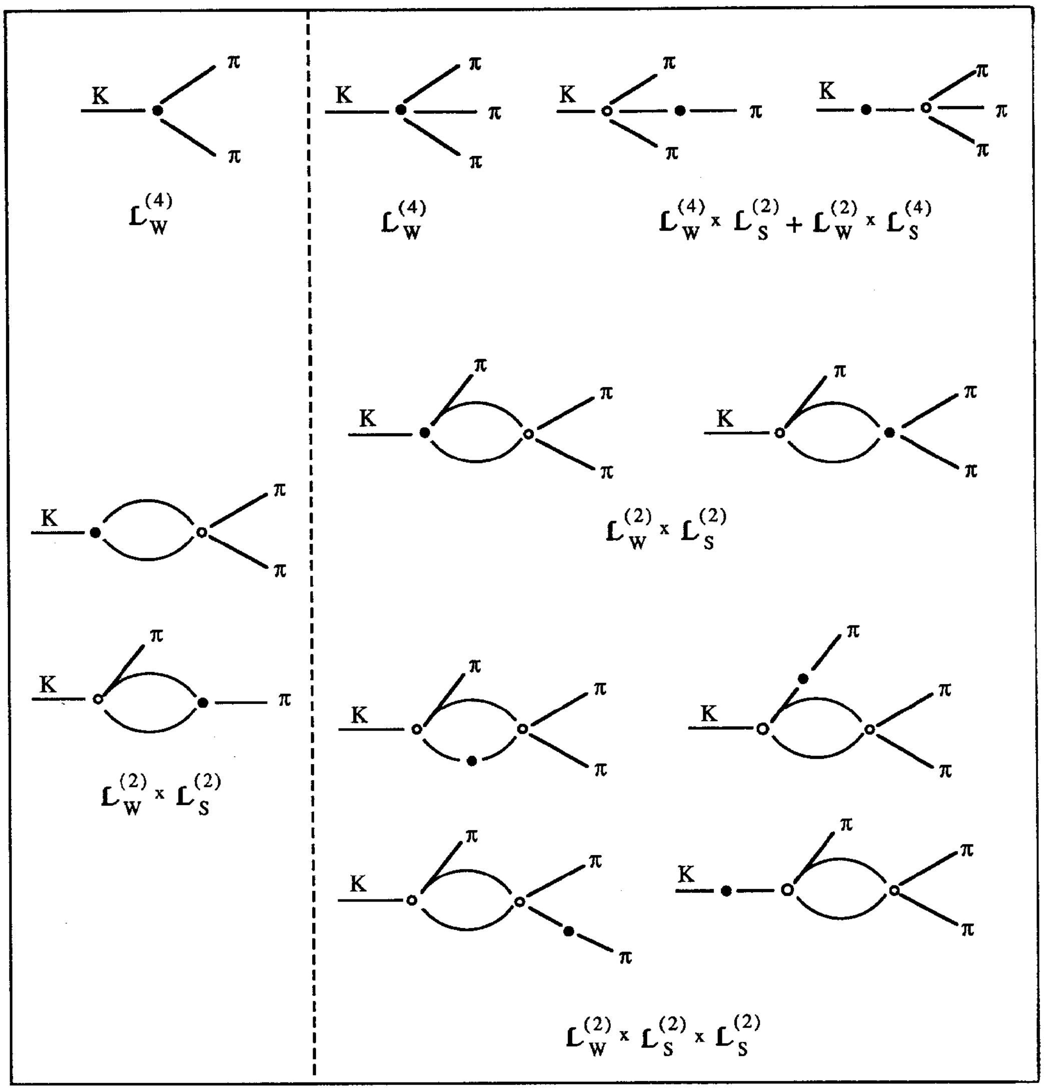

Figure 3: Examples of $O(p^4)$ contributions to $K \to 2\pi$ and $K \to 3\pi$: $\bullet$ and $\circ$ have the same meaning as in Fig. 2.

already available from the analyses of the strong interaction sector [21, 19], and therefore do not introduce anything unknown.

Counterterms regulate loop divergences, and in general both contributions separately depend (logarithmically) on a renormalization scale μ, such that their sum in (28) is scale-independent.

As for the structure of the seven weak counterterm contributions to the individual amplitudes, denoting their coupling constants by $K_1, \ldots, K_7$, neglecting the tiny $\Delta I = 1/2$ component of c_3 and (small) corrections of order m_π^2/m_K^2, and adding the lowest order Eqs. (24) and (25), one finds for the $\Delta I = 1/2$ $K \to 2\pi$ amplitude the complete expression [5, 25]:

$$a_{1/2,tree} = \sqrt{6}\frac{m_K^2}{F_\pi^2 F_K}\left(c_2 - \frac{2}{9}m_K^2 K_1\right), \tag{29}$$

and, absorbing the counterterm coupling K_1 in $c_2 \to c_2' = c_2 - \frac{2}{9}m_K^2 K_1$, for the $\Delta I = 1/2$ $K \to 3\pi$ amplitudes:

$$\begin{aligned} \alpha_{1,tree}^w &= \frac{1}{3}\frac{m_K^2}{F_\pi^3 F_K}\left(c_2' + \frac{2}{9}m_K^2 K_2\right), &\qquad \zeta_{1,tree}^w \equiv \zeta_{1,ct}^w &= -\frac{1}{6}\frac{m_\pi^4}{F_\pi^3 F_K}K_2, \\ \beta_{1,tree}^w &= -\frac{m_\pi^2}{F_\pi^3 F_K}\left(c_2' + \frac{1}{9}m_K^2 K_3\right), &\qquad \xi_{1,tree}^w \equiv \xi_{1,ct}^w &= -\frac{1}{6}\frac{m_\pi^4}{F_\pi^3 F_K}K_3. \end{aligned} \tag{30}$$

Likewise, in the $\Delta I = 3/2$ sector:

$$a_{3/2,tree} = -\frac{20}{\sqrt{3}}\frac{m_K^2}{F_\pi^2 F_K}\left(c_3 + \frac{1}{3}m_K^2 K_4\right), \tag{31}$$

and, absorbing the counterterm K_4 in the definition of $c_3 \to c_3' = c_3 + \frac{1}{3}m_K^2 K_4$:

$$\begin{aligned} \alpha_{3,tree}^w &= \frac{20}{9}\frac{m_K^2}{F_\pi^3 F_K}\left(c_3' + \frac{2}{3}m_K^2 K_5\right), &\qquad \zeta_{3,tree}^w \equiv \zeta_{3,ct}^w &= \frac{4}{3}\frac{m_\pi^4}{F_\pi^3 F_K}K_5, \\ \beta_{3,tree}^w &= \frac{25}{3}\frac{m_\pi^2}{F_\pi^3 F_K}\left(c_3' + \frac{m_K^2}{30}\widetilde{K}\right), &\qquad \xi_{3,tree}^w \equiv \xi_{3,ct}^w &= -\frac{5}{24}\frac{m_\pi^4}{F_\pi^3 F_K}\widetilde{K}, \\ \gamma_{3,tree}^w &= -\frac{15\sqrt{3}}{2}\frac{m_\pi^2}{F_\pi^3 F_K}\left(c_3' + \frac{1}{18}m_K^2 K_7\right), &\qquad \xi_{3,tree}'^w \equiv \xi_{3,ct}'^w &= \frac{15}{8}\frac{m_\pi^4}{F_\pi^3 F_K}K_7, \end{aligned} \tag{32}$$

where $\widetilde{K} = 4K_6 + 3K_7$. Eqs. (30)-(32) imply the following consistency conditions among the $O(p^4)$ weak counterterm contributions:

$$\zeta_{1,ct}^w = -\frac{9}{4}\frac{m_\pi^4}{m_K^4}\alpha_{1,ct}^w, \qquad \xi_{1,ct}^w = \frac{3}{2}\frac{m_\pi^2}{m_K^2}\beta_{1,ct}^w, \tag{33}$$

$$\zeta_{3,ct}^w = \frac{9}{8}\frac{m_\pi^4}{m_K^4}\alpha_{3,ct}^w, \qquad \xi_{3,ct}^w = -\frac{3}{4}\frac{m_\pi^2}{m_K^2}\beta_{3,ct}^w, \qquad \xi_{3,ct}'^w = -\frac{3\sqrt{3}}{2}\frac{m_\pi^2}{m_K^2}\gamma_{3,ct}^w. \tag{34}$$

The strategy followed by the authors of Ref. [5], to phenomenologically determine the weak coupling constants K_i, is to fit to the experimental data in Tabs. 4 and 5 the full theoretical structure of $K \to 2\pi$ and $K \to 3\pi$ isospin amplitudes up to order p^4, with the calculated one-loop diagrams and the determinations of strong counterterms of Ref. [21] as inputs.

The resulting numerical values of the weak counterterm constants, and of the calculated one-loop contributions, are presented in Ref. [5] for the renormalization scale $\mu = m_\eta$, which minimizes loop diagrams with intermediate kaons and etas. It is interesting that the $\Delta I = 1/2$ pattern, dominant at order p^2, turns out to be reproduced also at the order p^4 level by weak counterterms. The values of loops and counterterms at other renormalization scales, such as $\mu = m_\rho$ and $\mu = 1\,GeV$, can be found in Ref. [26], and show that the separate scale dependences of these contributions can be quite sizable.

In Tabs. 5 and 6 we report the numerical results of the above mentioned 'chiral fit' for the $K \to 2\pi$ and $K \to 3\pi$ amplitudes, respectively. From Tab. 5 it is important to notice that the renormalization of the octet and 27-plet coupling constants c_2 and c_3 from the order p^2 values, due to the $O(p^4)$ corrections, is substantial (about 30%) in the case of the former, while the latter remains practically unaffected. As for the $K \to 3\pi$ amplitudes, the comparison of the numbers in the third column of Tab. 6 with those in Tab. 4 shows that the theoretical structure including the next-to-leading chiral corrections is able to well-reproduce the constant and linear amplitudes for all channels, in particular to accomodate the phenomenological observation that such corrections should be somewhat larger in the $\Delta I = 3/2$ sector. Clearly, this is very encouraging and supports the chiral Lagrangian picture. On the other hand, due to the large experimental uncertainties, the situation for the quadratic slopes is not as well-defined, specially for the $\Delta I = 3/2$ ones which are expected to be suppressed, so that a real clarification should wait for better data.

In fact, in this regard, one could try to go beyond the global fitting procedure, and take advantage of the consistency relations (33) and (34) among weak counterterm contributions [25]. Once K_1 and K_4 are absorbed in the $K \to 2\pi$ amplitudes giving the new values of c_2 and c_3, and the remaining five weak counterterms are fitted from the (best determined) constant and linear $K \to 3\pi$ amplitudes, the quadratic amplitudes can be parameter-free predicted. Actually, these would represent the true, genuine predictions of χPT at $O(p^4)$, and accordingly provide the non-trivial test of this framework.

Such predictions for the quadratic amplitudes are reported in the fourth column of Tab. 6. The comparison with the determinations in Tab. 4 is remarkably successful for the $\Delta I = 1/2$ amplitudes. It is not as good for the $\Delta I = 3/2$ slopes. However, these are given by the difference of two (almost cancelling) large numbers, so that uncertainties can have a dramatic effect in this case. To give an idea, we notice that, for $K_L \to 3\pi^0$, the value of the Dalitz plot parameter h predicted by Tab. 6 combined with the expansion (15) would be $h = -(1.2 \pm 0.4) \times 10^{-2}$. Direct use of the determinations in Tab. 4 would give, instead, $h = -(1.2 \pm 3.6) \times 10^{-3}$, to finally compare with the recent experimental measurement reported in Tab. 2, $h = -(3.3 \pm 1.1 \pm 0.7) \times 10^{-3}$ [14]. Indeed, by combining their result with the experimental determinations of h for the charged kaon decay modes, the authors of [14] would find the rather large ratio of $\Delta I = 3/2$ to $\Delta I = 1/2$ amplitudes

$\zeta_3/\zeta_1 \simeq 0.3 \pm 0.10$. All this shows, on the one side, the crucial role of quadratic amplitudes, in particular of the $\Delta I = 3/2$ ones, as tests of the χPT framework, and, on the other side, that possible discrepancies should not be considered as conclusive at the present level of accuracy.

Therefore, further experimental work attempting to improve the determinations of $K \to 3\pi$ isospin amplitudes, in particular of the X^2 and the Y^2 terms, is required for more significant tests. In this regard, to substantially reduce theoretical uncertainties, more accurate determinations of the strong counterterms, dominating the pole diagram contributions in Fig. 3, should be extremely useful and would lead to more precise determinations of the weak counterterms. Also, the order p^4 is the leading one for quadratic amplitudes so that, in principle, their predicted values at this level stand on a less firm footing with respect to constant and linear terms. Therefore, uncertainties of the order of 20-40% from $O(p^6)$ corrections, affecting the predictions for quadratic terms in Tab. 6, should be kept in mind until some quantitative assessment of such higher order effects is available. Finally, in the quest of most reliable predictions, considering that substantial QED effects can possibly affect quadratic amplitudes [27, 28], further theoretical work should also be directed to improved estimates of isospin breaking corrections.

The order p^4 loop diagrams in Fig. 3, with on-shell propagators in internal lines, generate the final state interaction imaginary parts at the leading order. For $K \to 2\pi$ this mechanism generates the strong interaction relative phase $\delta_2 - \delta_0$ between the two isospin amplitudes. The determination of this phase obtained by the fit of Ref. [5], reported in Tab. 5, is in reasonable agreement with the value directly measured in π-π scattering, $\delta_2 - \delta_0 = -(47 \pm 6)^\circ$ [29], the small discrepancy being due to the neglect of isospin breaking and electromagnetic corrections in $K \to 2\pi$ amplitudes. From the fourth column of Tab. 5 we see that the leading order somewhat underestimates $\delta_2 - \delta_0$. This is not surprising, since in this channel the relevant π-π phase shifts are evaluated at $\sqrt{s} = m_K$, a rather high energy from the point of view of χPT, so that ones expects a large contribution from the next order in momenta [30].

As emphasized in the previous section, due to the small Q-values, final state interaction phases in $K \to 3\pi$ are much more directly relevant to the low-energy regime, where leading order calculations should be most reliable. Explicit expressions of rescattering at leading order in χPT can be found in [31, 22] and, in the framework of the rescattering matrix, in [12]. Numerical results for both real and imaginary parts of the loop amplitudes are also given in Ref. [5]. However, the explicit kinematical dependence is needed in addition, in order to unambiguously reconstruct the rescattering matrix. In particular, for the coefficients of the expansion around the centre of the Dalitz plot in Eq. (14), we find:

$$\begin{aligned}
\alpha_0 &= \frac{1}{32\pi F_\pi^2}\sqrt{1-\frac{4m_\pi^2}{s_0}}\,\left(s_0+m_\pi^2\right) \simeq 0.13 \\
\alpha_0' &= -\frac{5}{32\pi F_\pi^2}\sqrt{1-\frac{4m_\pi^2}{s_0}}\,\frac{m_\pi^2\,(s_0-2m_\pi^2)}{s_0-4m_\pi^2} \simeq -0.13 \\
\beta_0 &= -\delta_0 = \frac{1}{32\pi F_\pi^2}\sqrt{1-\frac{4m_\pi^2}{s_0}}\,\left(s_0-m_\pi^2\right) \simeq 0.047\,.
\end{aligned} \tag{35}$$

An experimental verification of these predictions would also be of relevance to the chiral test.[7]

5.2 Factorization and resonance exchange models

In order to complement the theoretical description and make it more predictive, it would be desirable to estimate the strong and weak counterterm couplings in the framework of QCD. There presently are some attempts to dynamically derive the values of these couplings from 'first principles', by means of suitable effective actions representing moderate-energy QCD, limited to the operators relevant to the strong interaction $\mathcal{L}_S^{(4)}$. Results seem encouraging [33], and hopefully will lead to an improved theoretical situation, at least in the strong interaction sector.

5.2.1 Large N_c calculations

A definite prediction for $O(p^4)$ coupling constants (both strong and weak ones) can be obtained by using the framework of chiral perturbation theory in the leading $1/N_c$ expansion ($N_c \to \infty$) and leading order α_s, N_c being the number of quark colors, combined with factorization. Basically, noting that the quark effective nonleptonic Hamiltonian (18) is of the *current* $\times$ *current* form, in this approach a 'bosonization' prescription is separately applied to each of the quark currents. For example, the left-handed currents, considered as Noether currents of the chiral symmetry of the QCD effective action, can be expanded in $O(p)$ plus $O(p^3)$ terms as:

$$J_\mu = \bar{q}_L \gamma_\mu q_L \Rightarrow -\frac{F_\pi^2}{2}\left[L_\mu + \frac{1}{\Lambda_\chi^2}(terms\ cubic\ in\ L_\mu) + (derivative\ terms)\right], \tag{36}$$

where L_μ has been defined previously, and Λ_χ is a scale characterizing chiral symmetry breaking (of the order of $1\,GeV$). An analogous bosonization could be written for right-handed current operators. Replacing Eq. (36) into the large N_c effective nonleptonic quark Hamiltonian [34], the chiral weak Lagrangian $\mathcal{L}_W$ assumes the factorized, *current* $\times$ *current* structure [35, 36]

$$\mathcal{L}_W(8_L, 1_R) = c_2\, Tr\, \lambda_6 J_\mu J^\mu, \tag{37}$$

and an analogous expression can be obtained for the 27-plet component.

The advantage of factorization, which is expected to hold in the large N_c approximation, is that the strong Lagrangian, *via* the bosonization prescription (36) of the chiral quark currents, uniquely determines the structure of $\mathcal{L}_W^{(4)}$. In particular, the unknown weak counterterms can be related to (known) strong counterterms. The additional advantage of the large N_c approximation is that, in this limit, the strong coupling constants can be predicted [37], so that the number of free parameters is reduced to a minimum. Numerical

[7] Actually, if measured, such imaginary parts should be relevant also to $\eta \to 3\pi$, as they would unitarize the leading order amplitude for that decay [32], because in this case mass and energy scales are almost the same as in $K \to 3\pi$.

results in the $1/N_c$ approach, from Refs. [35] and [36], are reported in Tab. 6. The comparison with the data seems encouraging, although, concerning the test in the $\Delta I = 3/2$ sector and the needed accuracies, the same comments hold as previously made with regard to Eqs. (33) and (34).

Although being quite predictive, the leading $1/N_c$ scheme has also some conceptual difficulties. For example, the results of Tab. 6 are obtained by employing the values of c_2 in Eq. (37), and of the corresponding 27-plet coupling constant c_3, measured from the experimental $K \to 2\pi$ data, instead of taking the (rather different) leading $1/N_c$ values of these coefficients. This opens the question of the quantitative role of next-to-leading $1/N_c$ corrections and nonfactorizable contributions [38], and of the convergence of the expansion for $N_c = 3$. Another point is that chiral loops are negligible at the leading order in $1/N_c$, hence strong rescattering phases vanish and must be included by hand. In the absence of meson loops, the counterterm coupling constants become mass-scale independent, so that the problem of the μ-dependence is not well-addressed and, at this order, the comparison with the results obtained in the full chiral Lagrangian theory is not unambiguous.

5.2.2 Resonance exchange model

Spin-zero and spin-one resonance exchange, with chiral invariant couplings between resonances and pseudoscalar mesons, is a phenomenological model which turns out to be numerically quite successful for the $O(p^4)$ strong interaction constants. Also, it improves the theoretical description, by giving a well-recognizable physical meaning to the counterterms. By construction, this determination of counterterms is μ-independent, so that, in principle, the comparison with the scale-dependent matrix elements of $\mathcal{L}_S^{(4)}$ has some ambiguity. Nevertheless, it was shown that meson exchanges almost entirely saturate those couplings, as being in good agreement with the values determined phenomenologically from experimental data in Ref. [21], if the scale μ is chosen between, say, m_ρ and $1\,GeV$ [39, 40]. This suggests that a similar meson-exchange dominance could work also for the weak constants needed in $\mathcal{L}_W^{(4)}$. However, while there exists enough information to experimentally determine the strong resonance couplings needed for the $\mathcal{L}_S^{(4)}$ counterterms, in the case of $\mathcal{L}_W^{(4)}$ the situation is complicated by the additional need of weak resonance couplings to pseudoscalar mesons, which are not known and can only be calculated within specific models. Clearly, as a common feature, the role of such models is to relate the weak $O(p^4)$ constants to the strong constants, the only ones which are known.

One possibility is represented by the factorization model previously introduced, which is based on independent 'bosonization' of the weak quark currents similar to Eq. (36), and leads to a factorized weak Lagrangian of the form in Eq. (37) (but with with finite $N_c = 3$). In this case, the strong counterterms needed in the next-to-leading terms are phenomenologically determined either directly from experiment or *via* the resonance exchange parametrization. More precisely, in the application of Ref. [26], to phenomenologically account for next-to-leading corrections in $1/N_c$ a free coefficient k_f is introduced in the factorized expression of $\mathcal{L}_W^{(4)}$, so that naive factorization would correspond to $k_f = 1$. Another proposed model is the so-called 'weak deformation model' [41], essentially based on (i) the observation that, at leading order p^2, the weak nonleptonic Lagrangian can be directly obtained from the strong one by means of a suitable transformation, called 'deformation', and (ii) the requirement that the same 'deformation' generates, more in general, also the higher order weak Lagrangian from the corresponding strong one. This model is found to be equivalent to the previous one for $k_f = 1/2$ [26]. Clearly, from the outset the above models for the weak constants do not refer to resonances. The latter are introduced once the strong couplings are saturated by resonance exchange.

Vector-meson dominance was initially considered in Ref. [42], limiting to the $(8_L, 1_R)$ component of the weak Hamiltonian. Due to Bose statistics, by their vectorial nature spin-one mesons can only contribute to the amplitudes β_1 and ξ_1, because they couple only to final states antisymmetric under exchange of two pions, so that only the constant K_3 in (30) would be nonzero, while $K_1 = K_2 = 0$. In addition, in the factorization model with only vector-meson exchange, also K_3 is found to vanish [42]. Therefore, having been determined phenomenologically to be non-zero within uncertainties [5], weak counterterms are likely not to be dominated by vector-meson exchange. This might signal a situation rather different from the strong interaction case.

Even limiting to the $(8_L, 1_R)$ component, the general structure of $\mathcal{L}_W^{(4)}$ including both spin-zero and spin-one resonance exchanges introduces too many weak resonance couplings, and no simplification of the $O(p^4)$ chiral structure of $\mathcal{L}_W^{(4)}$ would be obtained at the general stage, without assuming a model [26].

In the factorization model, where vectors do not contribute, finite values of the constants K_i can result only from spin-zero meson exchange, which would imply $K_1 < 0$ and $K_2 = K_3$ in Eq. (30). The phenomenologically determined constants do not seem to agree with these predictions. Furthermore, the size of $K_{1,2,3}$, predicted by using the scalar resonance couplings determined in Ref. [39], does not compare well with the phenomenological determinations, unless the value of k_f is chosen very far from unity. Interpreted pessimistically, this might indicate a trouble for the factorization model. However, such a comparison might not be completely conclusive yet, considering the uncertainties which affect the present determinations of the constants K_i. These uncertainties are induced by the experimental ones, and also in large part by the inaccuracies of the strong couplings determinations that are used as input in the 'chiral fit'. In addition, the strong scale-dependence of the K_i complicates the comparison with models at the present stage.[8]

6 Measurements at the ϕ factory

According to the previous considerations, accurate measurements of the $K \to 3\pi$ Dalitz plot for the individual channels would allow a stringent test of the current theoretical description of the $|\Delta S| = 1$ nonleptonic weak interaction, in particular of the chiral Lagrangian realization to order p^4. The determination of isospin amplitudes requires, in

[8]Numerical predictions for the $K \to 3\pi$ isospin amplitudes in the framework of factorization and resonance-exchange have been worked out in Ref. [43], choosing the (rather low) renormalization scale $\mu = m_\eta$ for loop contributions. The μ-dependence of the results is not discussed in this paper.

general, the combination of data on both $K^\pm$ and K^0 decays. DAΦNE is a source of pure kaon beams, free from background contaminations, which in principle should allow high statistical accuracy (see Tab. 1), provided that detection efficiencies for decay products are also high. However, in some cases the present experimental accuracy is mostly limited by systematic errors that must be decreased accordingly, in order to take advantage of the quality of kaon beams. Another source of difficulty, to be taken into account in $K \to 3\pi$ analyses, is the correlations among, e.g., linear and quadratic Dalitz plot slopes, which relate the accuracies obtainable for these parameters. The case of $K_L \to 3\pi^0$ is a special one, since the quadratic slope is not contaminated by the linear amplitude which is zero for this mode (see Eq. (14)), and electromagnetic corrections are not required.

The direct observation of many hundreds of $K_S \to \pi^+\pi^-\pi^0$ decay events, with practically no background (see Tab. 1), should represent a significant achievement obtainable at DAΦNE and, as pointed out previously, will allow to carefully test the $\Delta I = 3/2$ component of the weak Hamiltonian.

Another interesting analysis of $K^0 \to 3\pi$ is suggested by the use of DAΦNE as an 'interferometer', where the time dependence of K_L-K_S interference in vacuum can be accurately studied. Since the initial $K\bar{K}$ state from ϕ decay is the antisymmetric superposition

$$|i>\cong \frac{1}{\sqrt{2}}\left[|K_L(\hat{z})K_S(-\hat{z})\rangle - |K_S(\hat{z})K_L(-\hat{z})\rangle\right], \tag{38}$$

where $\hat{z}$ is the direction of the kaons momenta in the c.m. system, the subsequent K_L and K_S decays are correlated, and their quantum interferences show up in relative time distributions and time asymmetries, which are of great interest in order to test CP (and CPT) violation [44]. In addition, as an alternative to the direct observation, also the CP conserving $K_S \to \pi^+\pi^-\pi^0$ amplitude and the final state interaction imaginary parts could be measured *via* the time dependent interference of this decay with $K_L \to \pi^+\pi^-\pi^0$ [45, 12].

Specifically, a convenient observable is represented by the transition rate for the initial state $|i\rangle$ to decay into the final states $f_1 = \pi^\pm l^\mp \nu$ at time t_1 and $f_2 = \pi^+\pi^-\pi^0$ at time t_2, respectively (in the following, t_1 and t_2 are understood to be the proper times). Defining the 'intensity' of time correlated events $I(t)$ as:

$$I(t) = \frac{1}{2}\int_{|t|}^{\infty} d\tau\, |\langle f_1(t_1), f_2(t_2)|T|i\rangle|^2, \tag{39}$$

where $\tau = t_1 + t_2$ and t is the time difference $t = t_1 - t_2$, making use of the exponential time-dependence of the mass eigenstates K_S and K_L, and integrating over the $K^0 \to \pi l \nu$ phase space, one easily finds, with the notations $A_{S,L} \equiv A^{S,L}_{+-0}$:

$$\begin{aligned} I(\pi^\pm l^\mp\nu, \pi^+\pi^-\pi^0; t<0) &= \frac{\Gamma(K_L \to \pi l\nu)}{2\Gamma}\{|A_L|^2 e^{-\Gamma_L|t|} + |A_S|^2 e^{-\Gamma_S|t|} \pm 2e^{-\Gamma|t|} \\ &\times\ [\Re(A_L A_S^*)\cos(\Delta m|t|) + \Im(A_L A_S^*)\sin(\Delta m|t|)]\}, \end{aligned} \tag{40}$$

and

$$I(\pi^\pm l^\mp\nu, \pi^+\pi^-\pi^0; t>0) = \frac{\Gamma(K_L \to \pi l\nu)}{2\Gamma}\{|A_L|^2 e^{-\Gamma_S t} + |A_S|^2 e^{-\Gamma_L t} \pm 2e^{-\Gamma t}$$

$$\times \quad [\Re(A_L A_S^*)\cos(\Delta m t) - \Im(A_L A_S^*)\sin(\Delta m t)]\}. \tag{41}$$

In Eqs. (40) and (41), $\Gamma = (\Gamma_L + \Gamma_S)/2$, $\Delta m = m_L - m_S$, and for the $K \to 3\pi$ amplitudes the expansions (14) or (15) must be introduced. From these equations one can notice the possibility to study, in general, also negative 'times', which is peculiar of the ϕ factory [46].

An important aspect of the interference in (40) and (41) is that, besides the real parts, the (expectedly) small final state interaction imaginary parts appear linearly. Instead, the width depends quadratically on them and thus has less sensitivity to such effects. Accordingly, by a fit to the full t-dependence of the interference, both the real and the imaginary parts could be determined (or at least, for the latter ones, a significant upper bound could be obtained, depending on the available statistics). This would be a desirable achievement, in view of the discussion in Sec. 3.

Using Eq. (14) or (15), the interference terms are easily seen to drop from the intensities (40) and (41) integrated over the full $K \to 3\pi$ Dalitz plot, giving the total event rates. Considering that in the CP conserving case the Dalitz plot distributions are even in X for all channels, the interference can be extracted by integrating the intensities (40) and (41) over the $K \to 3\pi$ phase space with odd-X cuts.

For example, with $d\Phi$ the phase space element, one can define the asymmetries

$$R_X^{\pm}(t) = \frac{\int d\Phi\, \mathrm{sgn}(X)\, I(l^{\mp}\pi^{\pm}\nu, \pi^+\pi^-\pi^0; t)}{\int d\Phi\, I(l^{\mp}\pi^{\pm}\nu, \pi^+\pi^-\pi^0; t)}, \tag{42}$$

and

$$R_{XY}^{\pm}(t) = \frac{\int d\Phi\, \mathrm{sgn}(XY)\, I(l^{\mp}\pi^{\pm}\nu, \pi^+\pi^-\pi^0; t)}{\int d\Phi\, I(l^{\mp}\pi^{\pm}\nu, \pi^+\pi^-\pi^0; t)}. \tag{43}$$

Using Eq. (14) to expand $\Re(A_L A_S^*) \cong \Re A_L \Re A_S$ and $\Im(A_L A_S^*) = \Re A_S \Im A_L - \Re A_L \Im A_S$ up to second order in the kinematical variables, one finds to a good approximation

$$R_X^{\pm}(t>0) = \mp\frac{4}{3}e^{-\Gamma t}\frac{a_n b_2\, [\cos(\Delta m t) - \delta_X \sin(\Delta m t)]\int d\Phi\, |X|}{\int d\Phi\, [|A_L|^2 e^{-\Gamma_S t} + |A_S|^2 e^{-\Gamma_S t}]}, \tag{44}$$

where

$$\delta_X = \alpha_0 - \delta_0. \tag{45}$$

The amplitude a_n (and b_n) can be measured from the rates. Therefore, Eq. (44) shows that the separate determination of the $\cos(\Delta m t)$ and $\sin(\Delta m t)$ dependences allows the measurement of the $K_S \to \pi^+\pi^-\pi^0$ amplitude b_2, as well as of the rescattering relative phase $\alpha_0 - \delta_0$. In particular, the leading order χPT predictions in Eq. (35) indicate $\delta_X \simeq 0.18$.

The expression for $R_X^{\pm}(t<0)$ is directly obtained from (44) by the changes $t \to |t|$, $\delta_X \to -\delta_X$ and $\Gamma_L \leftrightarrow \Gamma_S$ but, as a function of time, the denominator would quickly become large and suppress the interference.

Analogously, $R_{XY}^{\pm}$ is given by the more complicated expression:

$$\begin{aligned} R_{XY}^{\pm}(t>0) &= \pm\frac{4}{3}e^{-\Gamma t}\frac{(b_n b_2 + 2a_n d_2)\int d\Phi\, |XY| - a_n b_2 \int d\Phi\, |X|\mathrm{sgn}(Y)}{\int d\Phi\, [|A_L|^2 e^{-\Gamma_S t} + |A_S|^2 e^{-\Gamma_L t}]} \\ &\times \quad [\cos(\Delta m t) - \delta_{XY}\sin(\Delta m t)], \end{aligned} \tag{46}$$

where

$$\delta_{XY} = \frac{\beta_0 - \delta_0 + \frac{a_n}{b_n}\left(\alpha_0' + 2\frac{d_2}{b_2}\alpha_0\right) - \frac{a_n}{b_n}\left(\alpha_0 - \delta_0\right)\rho}{1 + 2\frac{a_n}{b_n}\frac{d_2}{b_2} - \frac{a_n}{b_n}\rho}, \tag{47}$$

and

$$\rho = \frac{\int d\Phi\, |X| \mathrm{sgn}(Y)}{\int d\Phi\, |XY|}. \tag{48}$$

If separately determined, the coefficients of the $\cos(\Delta m t)$ and $\sin(\Delta m t)$ terms could be useful to constrain the value of the quadratic amplitude d_2 and the combination of imaginary parts in (47). In this regard, we can notice that the expectedly small d_2 has a large coefficient proportional to a_n/b_n (see Tab. 4). In fact, to leading order in χPT, the numerator in Eq. (47) must be of order p^2 (the same counting applies to δ_X), so that for theoretical consistency d_2, which is of order p^4, should not be included. In that case, Eq. (47) simplifies considerably, and using Eq. (35) we would predict $\delta_{XY} \simeq 0.30$ [12].

In conclusion, studies of the time-dependent interference described above should provide alternative measurements of the CP conserving $K^0 \to 3\pi$ amplitude, and eventually could also give indications on rescattering phases and test the relevant predictions. A quantitative discussion for DAΦNE, taking into account also the background from the CP even $(K^0\bar{K}^0)$ state due to the radiative decay $\phi \to K^0\bar{K}^0\gamma$, is presented in Ref. [44].

References

[1] Review of Particle Properties, Phys. Rev. D **50** (1994).

[2] A. Kreutz et al., Zeit. Phys. C **65** (1995) 67.

[3] G.B. Thomson et al., Phys. Lett. **B337** (1994) 411.

[4] T. Ruf, talk given at the 27th Int. Conf. on High Energy Physics, Glasgow, July 1994, to appear in the proceedings.

[5] J. Kambor, J. Missimer and D. Wyler, Phys. Lett. **B261** (1991) 496.

[6] See, e.g., T.D. Lee and C.S. Wu, Ann. Rev. Nucl. Sci. **16** (1966) 511.

[7] G. Amelino-Camelia, F. Buccella, G. D'Ambrosio, A. Gallo, G. Mangano and M. Miragliuolo, Zeit. Phys. C. **55** (1992) 63.

[8] C. Zemach, Phys. Rev. **133** (1964) 1201.

[9] S. Weinberg, Phys. Rev. Lett. **17** (1966) 61.

[10] T.J. Devlin and J.O. Dickey, Rev. Mod. Phys. **51** (1979) 237.

[11] For a review see, e.g., L. Maiani and N. Paver, this Handbook.

[12] G. D'Ambrosio, G. Isidori, N. Paver, A. Pugliese, Phys. Rev. D **50** (1994) 5767.

[13] See, e.g., L.F. Li and L. Wolfenstein, Phys. Rev. D **21** (1980) 178.

[14] Fermilab $E731$ Collaboration, S.V.Somalwar et al., Phys. Rev.Lett. **68** (1992) 2581.

[15] Y. Hara and Y. Nambu, Phys. Rev. Lett. **16** (1966) 875; C. Bouchiat and P. Meyer, Phys. Lett. **25B** (1967) 282.

[16] F.J. Gilman and M.B. Wise, Phys. Rev. D **20** (1979) 1216.

[17] For an introduction and updated references see, e.g., M. Ciuchini, E. Franco, G. Martinelli and L. Reina, this Handbook.

[18] J.A. Cronin, Phys. Rev. **161** (1967) 1483.

[19] For a review see, e.g., J. Bijnens, G. Ecker and J. Gasser, this Handbook.

[20] J. Kambor, J. Missimer and D. Wyler, Nucl. Phys. **B346** (1990) 17.

[21] J. Gasser and H. Leutwyler, Ann. Phys. (N.Y.) **158** (1984) 142; Nucl. Phys. **B250** (1985) 465, 517.

[22] G. Isidori, L. Maiani and A. Pugliese, Nucl. Phys. **B381** (1992) 522.

[23] J.F. Donoghue, Nucl. Phys. **B** (Proc. Suppl.) **7A** (1989) 59, and references there.

[24] G. D'Ambrosio, G. Ecker, G. Isidori and H. Neufeld, this Handbook.

[25] J. Kambor, J.F. Donoghue, B. Holstein, J. Missimer and D. Wyler, Phys. Rev. Lett. **68** (1992) 1818.

[26] G. Ecker, J. Kambor and D. Wyler, Nucl. Phys. **B394** (1993) 101.

[27] A. Neveu and J. Scherk, Phys. Lett. **27B** (1968) 384.

[28] W.T. Ford et al., Phys. Lett. **38B** (1972) 335.

[29] W. Ochs, πN Newletters **3** (1991) 25.

[30] J. Gasser and U.G. Meissner, Phys. Lett. **B258** (1991) 219.

[31] B. Grinstein, S.J. Rey and M. Wise, Phys. Rev. D **33** (1986) 1495.

[32] J. Gasser and H. Leutwyler, Nucl. Phys. **B250** (1985) 539.

[33] For reviews see, e.g., J. Bijnens, this Handbook; E. Pallante and R. Petronzio, this Handbook.

[34] W.A. Bardeen, A.J. Buras and J.-M. Gérard, Phys. Lett. **B192** (1987) 138; Nucl. Phys. **B293** (1987) 787.

[35] H.Y. Cheng, Phys. Lett. **B238** (1990) 399; Phys. Rev. D **42** (1990) 3850.

[36] S.Fajfer and J.-M.Gérard, Zeit. Phys. **C42** (1989) 425.

[37] D. Espriu, E. de Rafael and J. Taron, Nucl. Phys. **B345** (1990) 22, (E) **B355** (1990) 278; and references there.

[38] A. Pich and E. de Rafael, Nucl. Phys. **B358** (1991) 311.

[39] G. Ecker, J. Gasser, A. Pich and E. de Rafael, Nucl. Phys. **B321** (1989) 311.

[40] J.F. Donoghue, C. Ramirez and G. Valencia, Phys. Rev. D **39** (1989) 1947.

[41] G. Ecker, A. Pich and E. de Rafael, Phys. Lett. **B237** (1990) 481.

[42] G. Isidori and A. Pugliese, Nucl. Phys. **B385** (1992) 437.

[43] S. Fajfer, Zeit. Phys. C **61** (1994) 645.

[44] For a review and references see G. D'Ambrosio, G. Isidori and A. Pugliese, this Handbook.

[45] G. D'Ambrosio and N. Paver, Phys. Rev. D **46** (1992) 352; Phys. Rev. D **49** (1994) 4560.

[46] M. Fukawa et al., Physics at a ϕ factory, KEK Report 90-12 (1990).